STABILITY LIMITS AND DYNAMICS OF NONAXISYMMETRIC LIQUID BRIDGES.

J. Iwan D. Alexander[1], Lev A. Slobozhanin[2], Andrew H. Resnick[2], Jean-Francois Ramus[2] and Sylvie. Delafontaine[2]

[1]National Center for Microgravity Research and Department of Mechanical and Aerospace Engineering, Case Western Reserve University, Cleveland, OH 441106; [2]Center for Microgravity and Materials Research, University of Alabama in Huntsville, Huntsville, AL 35899

Abstract

Liquid bridges have been the focus of numerous theoretical and experimental investigations since the early work by Plateau more than a century ago. More recently, motivated by interest in their physical behavior and their occurrence in a variety of technological situations, there has been a resurgence of interest in the static and dynamic behavior of liquid bridges. Furthermore, opportunities to carry out experiments in the near weightless environment of a low-earth-orbit spacecraft have also led to a number of low-gravity experiments involving large liquid bridges. In this paper we present selected results from our work concerning the stability of nonaxisymmetric liquid bridges, the bifurcation of weightless bridges in the neighborhood of the maximum volume stability limit, isorotating axisymmetric bridges contained between equidimensional disks and bridges contained between unequal disks. For the latter, we discuss both theoretical and experimental results. Finally, we present results concerning the stability of axisymmetric equilibrium configurations for a capillary liquid partly contained in a closed circular cylinder.

1. Introduction

Liquid bridges occur in a number of different situations of physical and technological interest. The study of axisymmetric equilibria has received much attention and the stability of static bridges has been examined for various disk configurations, aspect ratios, gravity levels and rotation rates (see, for example, [1-7] and references therein.). There have also been numerous investigations of liquid bridge dynamics (e.g., [8,9]). Such investigations have been motivated by both practical considerations and basic scientific interest. The behavior of liquid bridges and drops are important considerations in propellant management problems and other fluid management problems in space [10, 11]. Pendular liquid bridges occur widely in the powder technology industry and are a major influence on powder flow processes and mechanical properties [12-13]. In porous media flow, liquid-liquid displacement can lead to evolution of pendant and sessile lobes or a lenticular bridge [13]. The formation of liquid bridges from the gel that coats lung micro-airways is a precursor in lung collapse [14]. The results for unequal diameter supports presented here are particularly relevant to floating zone crystal growth [7,15,16], since this is a common configuration [15, 16].

2. Nonaxisymmetric Bridge Stability

The stability of two types of static nonaxisymmetric bridge configurations was considered. In both cases, the bridge was held between equidimensional coaxial disks. In the first example, the stability of bridges subject to gravity oriented perpendicular to the axis through the supporting disks was examined. The second example dealt with nonaxisymmetric bridges subject to axial acceleration. Both problems were solved numerically using the *Surface Evolver code* [17].

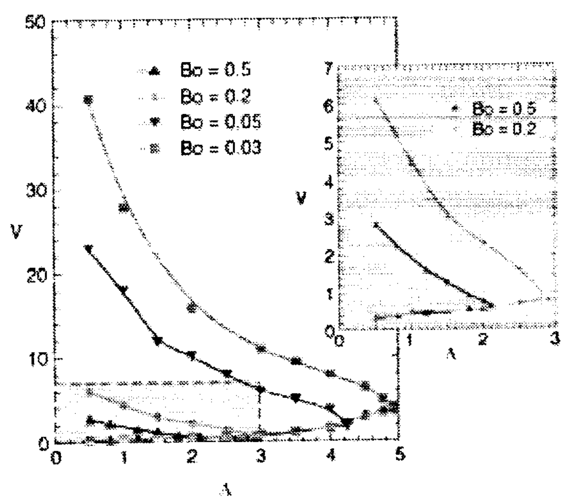

Fig. 1 Computed stability limits for lateral acceleration with Bo = 0.5, 0.2, 0.05 and 0.03.

The stability of bridges subject to lateral gravity was examined as a function of slenderness, Λ (ratio of the disk separation to the mean diameter, $2r_0$, of the two support disks), and the relative volume, V (ratio of the actual liquid volume to the volume of a cylinder with a radius r_0). The location of the stability boundary for a given Bond number, B, was determined by fixing the slenderness, Λ, and minimizing the energy for some value of V. Outside the stability boundary, the bridges break before the energy is minimized. Inside the stability boundary, bridges maintain their integrity and reach a minimum energy configuration. Thus, we employed a simple iterative search technique to find the approximate location of the boundary. For a given B and a fixed value of Λ that is less than the maximum stable slenderness, Λ_{max}, there exists a maximum and minimum stable relative volume. The maximum volume stability limit tends to infinity as $\Lambda \rightarrow 0$.

For any given (lateral) B, the minimum volume stability limit becomes indistinguishable from the zero B limit when Λ becomes sufficiently small. A more detailed description of these results is given in Ref. [18]

In related work carried out in collaboration with Prof. J. Meseguer and Dr. F. Zayas of the Universidad Politecnica de Madrid, we examined the results of an asymptotic analysis of the stability limits of liquid bridges. Here the maximum stable slenderness, $\Lambda_{\max}$, of a liquid bridge between equal disks, and a nearly cylindrical volume, when subjected to both axial (B_a) and lateral (B_l) Bond numbers becomes

$$b_l = (1 - (b_a)^{2/3})^{1/2}, \quad (1)$$

where

$$b_a = (3/2)^2 \lambda^{-3/2} B_a, \text{ and } b_l = (\pi/2)\lambda^{-1/2} B_l, \quad (2)$$

are the reduced axial and lateral Bond numbers and $\lambda = 1 - \Lambda_{\max}/\pi + v/2$, where $v = V - 1$. This suggests that, at least close to the reference configuration ($\Lambda \sim \pi$, $v \sim 0$, $B_a \sim 0$, $B_l \sim 0$), there is a self-similar solution for the stability limits, the behavior being the same regardless of the slenderness or volume. Numerical results obtained using *Surface Evolver* [17] were found to be in good agreement with Eq. (1) for a limited parameter range.

For axisymmetric bridges subject to axial gravity, it is known that along most of the maximum volume stability limit axisymmetric bridges are unstable to nonaxisymmetric perturbations. We examined the bifurcation of solutions for a weightless liquid bridge in the neighborhood of this stability boundary. Depending on the system parameters, loss of stability with respect to nonaxisymmetric perturbations resulted in either a jump or a continuous transition to stable nonaxisymmetric shapes. The value of the slenderness at which a change in the type of transition occurred was found to be $\Lambda_s = 0.4946$. Results of experiments using a neutral buoyancy technique agree with this prediction. A liquid bridge of a set slenderness was formed between coaxial disks. High precision stepping motors were used to control the disk separation while simultaneously injecting silicone oil. Oil was injected until the bridge was near the upper stability limit for the slenderness under consideration. Then precisely controlled amounts of oil were added incrementally using a calibrated microsyringe. The shape was monitored as the bridge expanded and stability limit was approached. The bridge was imaged using a coherent high magnification Fourier optical arrangement together with a high pass optical filter. This permits visualization of edges of projections of the liquid bridge surface at approximately 100x magnification. From this image, the minimum distance l (shown schematically in the photographs in Fig. 2) from the bridge surface to a stationary reticule was measured on a computer screen. Typically, the distance decreases slightly with each addition of oil until the stability limit is exceeded. When this occurs, the bridge forms a bulge. After loss of stability, the critical axisymmetric shape changes to a stable nonaxisymmetric shape. However, the nature of this transition was quite different for $\Lambda \leq 0.4$ and $\Lambda \geq 0.6$.

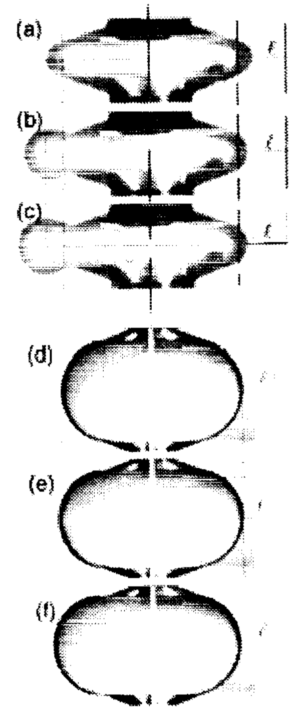

Fig. 2 Bridge images for $\Lambda = 0.225$ (*a - c*) and $\Lambda = 1.02$ (*d - f*). States (*a*) and (*d*) are stable and axisymmetric with $V_1 = 1.31$ and $V_2 = 2.82$ that are, respectively, slightly smaller than the critical (experimental) volumes for the given Λ. The nonaxisymmetric bridges (*b*) and (*c*) have $V = V_1 + 0.025$ and $V_1 + 0.05$, (*e*) and (*f*) have $V = V_2 + 0.095$ and $V_2 + 0.19$.

Figure 2 shows a sequence of images of a $\Lambda = 0.225$ bridge near the critical V value. The theoretically predicted critical volume is 1.36, the critical volume obtained experimentally was 1.33. For $\Lambda = 0.225$, a large shape deformation occurs after the addition of only a small volume increment (compare Figs. 2(a) and 2(b)). Further volume increases lead to continuous incremental shape changes (Figs. 2(b) and 2(c)). In contrast, for $\Lambda = 1.02$ (Figs. 2(d)-2(f)), we observed a continuous transition from critical axisymmetric shape to a sequence of the stable nonaxisymmetric shapes as the volume was increased. Here the theoretical critical volume is 2.96 and our experimental critical volume was between 2.83 and 2.85. In both cases, our experimental critical volumes were within 5% of the theoretical values and the nonaxisymmetric bridges were stable at volumes far beyond the maximum volume stability limit for axisymmetric bridges.

This work is described in detail in Refs. [19,20].

For bridges between coaxial disks and subject to axial gravity, little is known about the stability of nonaxisymmetric configurations beyond the maximum (axisymmetric) volume limit. We examined the stability of these bridges numerically (using *Surface Evolver*) for $B = 0.1$ and 2. We found that the maximum volume segment of the stability limit follows the same trend as for lateral gravity. That is, V tends to infinity as the slenderness, Λ , tends to zero.

3. Stability of Isorotating Liquid Bridges

The stability of axisymmetric equilibrium states of an isorotating liquid bridge between equidimensional circular disks in a constant axial gravity field was also considered [21]. Emphasis was given to the stability of bridges satisfying two types of constraint that are typical for the floating zone method used for materials purification and single crystal growth. First, we considered the constraint that the relative volume of the bridge, V, is equal to 1. For this case, the critical values of the slenderness (Λ) and of the surface slopes (β_1, β_2) at both disks have been determined for a wide range of the Bond and Weber (W) numbers. Figure 3 shows the level lines of the slope angle at the top and bottom disks ($\beta_1 = \beta_2$) for the critical surfaces of a cylindrical volume bridge. These curves lie in the region of the (, Λ)-plane enclosed by the $B = 0$ and $B = 5$ (dot-dash line) stability boundaries.

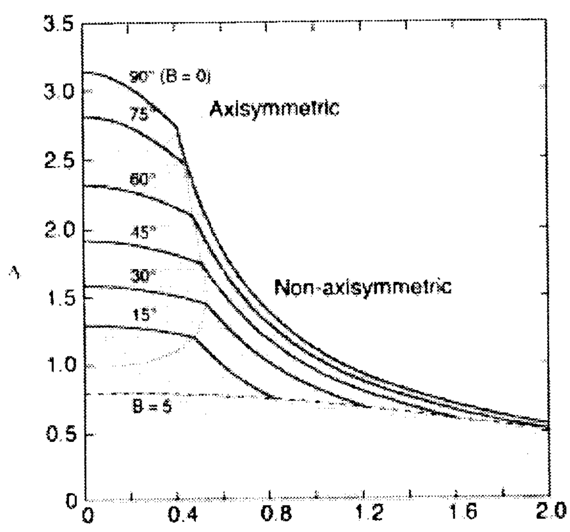

Fig. 3 Level lines of the slope angle at the top and bottom disks ($\beta_1 = \beta_2$) for the critical surfaces of a cylindrical volume bridge. The regions of critical axisymmetric and nonaxisymmetric perturbations are shaded green and yellow, respectively.

The second constraint considered is that the surface slope β_1 at one of the disks is prescribed. The chosen values were 90° and 75°. These values correspond to extremes in growth angle values encountered in floating zone crystal growth. For this case, the dependencies of critical Λ and V values on B and W were calculated. In addition, both axial gravity directions (i.e., up and down) were considered separately and the values of the slope angle, β_2, at the other disk were also analyzed for critical states.

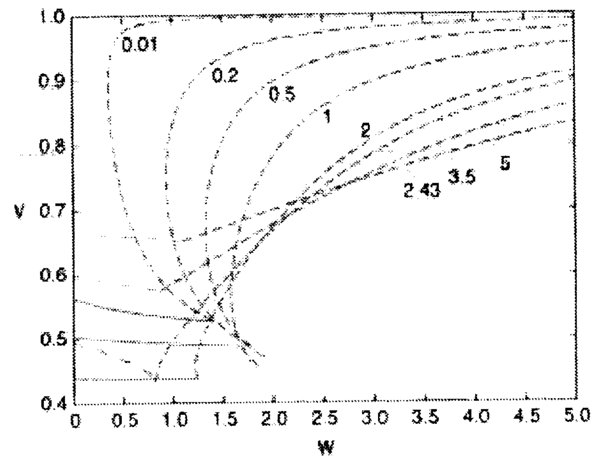

Fig. 4 Stability diagrams for bridges with $\beta_1 = 90°$ in the (W, V)-plane. Numbers on curves denote values of the positive Bond number (i.e. gravity acts such that β_1 is the surface slope at the lower disk, B. Solid (dashed) lines represent segments that correspond to states with critical axisymmetric (nonaxisymmetric) perturbations. Dot-dash lines represent states with limiting surfaces [21].

The solution of the stability problem for any axisymmetric isorotating liquid bridge between equal disks is discussed in detail using the case for $B = W = 0.1$ as an example. In particular, the relationship between the general boundary of the stability region and the stability of bridges subject to the constraints outlined above is examined. The stability region in the (Λ , V)-plane can also be constructed for any fixed pair of values of B and W. Examples of such regions are shown in Fig. 5.

The curves *1*, *2*, *3* and *4* represent the stability region boundaries for the cases of $B = W = 0$; $B = 0.1$, $W = 0$; $B = 0$, $W = 0.1$ and $B = W = 0.1$. Curves 2 and 3 illustrate the independent effects of gravity and centrifugal force. Each of these forces narrows the stability region as compared to the case $B = W = 0$. However, the shapes of the stability regions are different due to the different nature of the gravitational and centrifugal forces. Curve *4* illustrates the combined effect of these forces. As expected, the stability region for their combined action belongs to the intersection of the stability regions for their independent action.

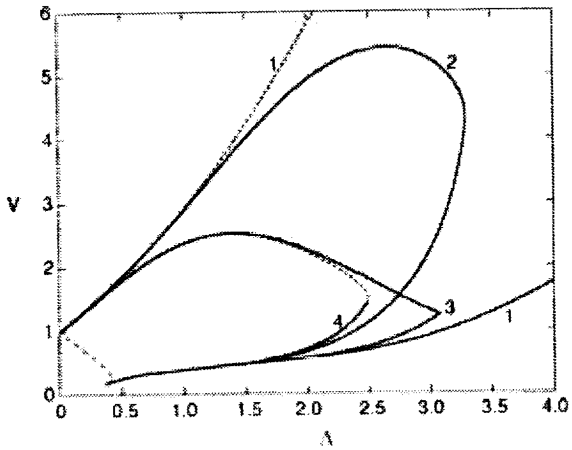

Fig. 5 General boundaries of the stability region for the cases: (1) $B = W = 0$; (2) $B = 0.1$, $W = 0$; (3) $B = 0$, $W = 0.1$; (4) $B = W = 0.1$. States critical to axisymmetric (nonaxisymmetric) perturbations are denoted by solid (dashed) lines.

The shapes of the boundaries *2*, *3* and *4* are typical for moderate values of B and W. Along the upper parts of all boundaries *1* - *4*, stability is lost to nonaxisymmetric perturbations. The lower part of each boundary consists of two segments separated by a cusp-point. On the right-hand segment, loss of stability occurs with respect to axisymmetric perturbations. The left-hand segments of these boundaries merge. However, the nature of the related critical states may be different. The entire left-hand segments of the curves *1* and *2* are determined by states with limiting surfaces. For curve *1*, these limiting surfaces are also the critical ones with respect to nonaxisymmetric perturbations. For an isorotating bridge (the curves *3* and *4*), only a part of this segment closer to the point (0, 1) is determined by states with limiting surfaces. The other part corresponds to states that are critical to nonaxisymmetric perturbations. If at least one of the parameters B and W is reasonably large, there is no neutrally stable state that is critical with respect to axisymmetric perturbations. Here the boundary points correspond either to neutrally stable surfaces that are critical with respect to nonaxisymmetric perturbations or to limiting surfaces.

Figure 6 shows the values of Λ and V for families of stable states, and for some unstable states, that have fixed values of β_1 or β_2. The stability boundary is curve *4* of Fig. 5. For stable states with $\beta_2 = 90°$ or $\beta_2 = 105°$ the Λ values lie between 0 and the critical value $\Lambda = \Lambda^*$. Values of V are bounded by 1 and the critical value $V = V^*$. Λ^* and V^* are determined by the point of intersection of $\beta_2 = const.$ and the general stability boundary. This point corresponds to the state that is neutrally stable to nonaxisymmetric perturbations and represents a "pitch-fork" bifurcation point. The construction of a level line $\beta_1 = const.$ or $\beta_2 = const.$ in the (Λ, V)-plane is important for determining the values of Λ and V for a stable bridge with a prescribed slope angle at one of disks. Finally, we note that the critical slenderness for a cylindrical volume bridge is determined by the point of intersection of the (dot-dash) line $V = 1$ and the general boundary.

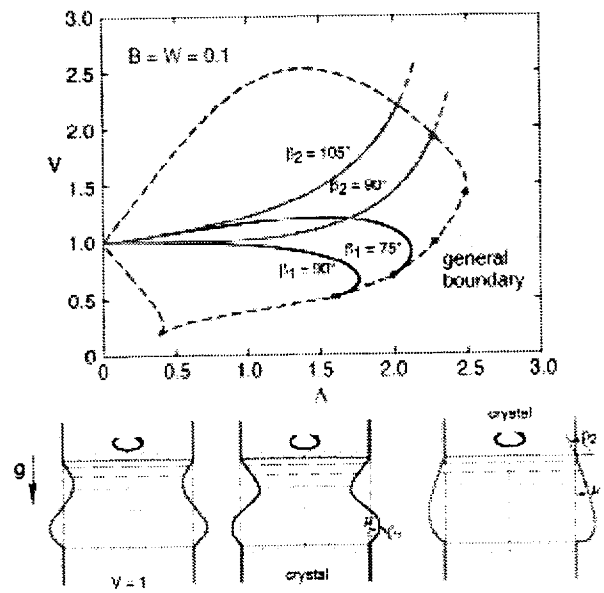

Fig. 6 Values of the slenderness, Λ, and the relative volume, V, for the stable (solid lines) and unstable (dotted lines) bridges with prescribed values of β_1 or β_2. The dashed line is the general boundary of the stability region for $B = W = 0.1$. The critical points are denoted by "open circles" and the transition point between axisymmetric and nonaxisymmetric dangerous perturbations by "closed circles".

4. Effect of Unequal Disk Radii on Stability

The stability of an axisymmetric liquid bridge between unequal circular disks in an axial gravity field was examined for all possible values of the liquid volume and disk separation. The parameter defining the disk inequality is K, the ratio between the radii of the smaller and larger disks. Both axisymmetric and nonaxisymmetric perturbations were considered.

The Λ -V plane was chosen as the appropriate parameter space to delimit the stability regions. Wide ranges of the B and K were considered. Emphasis was given to previously unexplored parts of the stability boundaries. In particular, we examined the maximum volume stability limit for bridges of arbitrary Λ and the minimum volume stability limit for small Λ bridges. The maximum volume stability limit was found to have two distinct properties: large values of the critical relative volume at small Λ, and the possibility that stability is lost to axisymmetric perturbations at small K. For a given set of K, we determined the maximum Bond number beyond which stability is no longer possible for any combination of V and Λ. We also obtained the maximum value of the actual liquid volume of a stable bridge that can be held between given disks for all possible disk separations for fixed B. It was found that this volume decreases as K decreases and (depending on the sign of B) tends to the critical volume of a sessile or pendant drop attached to the larger disk.

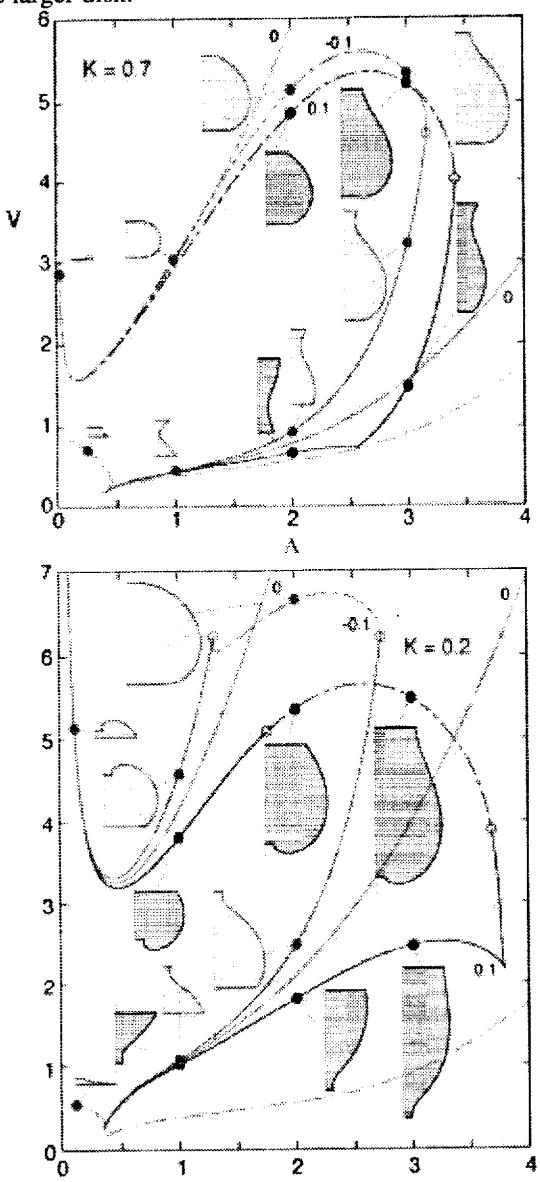

Fig. 7 Shapes of critical liquid bridge surfaces under a downward-directed axial gravity.

Figure 7. shows selected results for K =0.2 and 0.7. The Bond number is positive (negative) when the smaller disk is above (below). The corresponding states are marked by filled circles on the general stability boundaries for: (a) $K = 0.7$, $B = \pm 0.1$; (b) $K = 0.2$, $B = \pm 0.1$. Numbers on curves denote values of B. Solid (dashed) lines correspond to states critical to axisymmetric (nonaxisymmetric) perturbations. Dotted lines represent states with limiting surfaces, and the dot-dash line is the minimum volume stability limit for zero-gravity bridges between equal disks ($K = 1$, $B = 0$). A filled circle corresponds to the state with $\Lambda = \Lambda_{max}$ for a given stability boundary. Open circles represent transition points between different types of boundary segments (e.g., when states critical to axisymmetric perturbations become critical to nonaxisymmetric perturbations or change to states with limiting surfaces). Experimental results [20] are in good agreement with the results predicted by this analysis.

Finally, we present results concerning the stability of axisymmetric equilibrium configurations of a capillary liquid in a circular cylindrical container with planar ends that are orthogonal to a cylindrical wall. The liquid either is subject to an axial gravity field or is under zero-gravity conditions. We consider *doubly connected* free surfaces (i.e., they do not cross the cylinder's axis of symmetry) that bound an annular region occupied by the gas. This study was motivated by the problem of partly contained melts in low gravity solidification experiments. Preliminary results prove that a free surface with one of contact lines on one of the cylinder's planar ends and the other on a lateral wall is always unstable if the wetting angle, α, lies in the range $0 \le \alpha \le 90°$. The stability regions for this configuration have been constructed in the plane "$\alpha - V$" (here $V = v_g/r_0^3$ is the relative gas volume) for set values of the B in the interval $-10 \le B \le 60$. It has been established that the stability region is connected if $B > B_0$ or $B < B_1$ ($-1.69 > B_0 > -1.70$ and $-1.79 > B_1 > -1.80$). If $B_1 < B < B_0$, the stability region consists of two disconnected parts. It was also found that a doubly connected free surface with both contact lines on a cylindrical wall may exist only under zero-gravity conditions (see Fig. 8). Further analysis revealed that only unduloidal free surfaces with profiles that contain inflection points may be stable to nonaxisymmetric perturbations. Such a free surface may be stable to arbitrary perturbations if $\alpha > 121°$. For a given $121° < \alpha < 180°$, the minimum and maximum stability limits of the relative gas volume have been determined.

Two special liquid bridge type configurations were also analyzed. One with a free surface pinned to edges of both end plates of a cylinder and the other with one part of the free surface pinned to edges of a cylinder's planar end and the other to a solid rod contained within the cylinder. This problem is connected with a new technique for "contactless" directional crystallization in low gravity. We analyzed stability conditions for the first configuration at $B = 0$ and $B = 0.05$, and arbitrary values of other parameters (wetting angles, aspect ratio and the liquid relative volume). Similar results have been obtained for the second configuration for rod/cylinder radius ratios equal to 0.8 and 0.6.

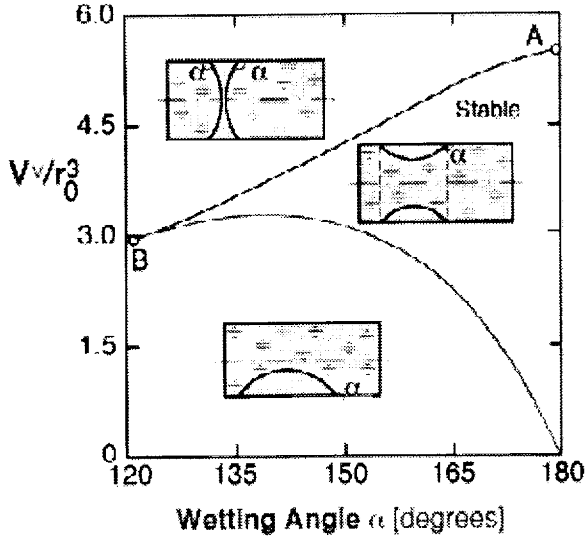

Fig. 8 Dependence of the vapor relative volume, $V^v = V^v/r_0^3$, on the wetting angle, α, for critical states of configurations with contact lines on the lateral wall of the cylinder.

Acknowledgments

This work was supported by the National Aeronautics and Space Administration through grant NAG3-1384.

References

1. L. A. Slobozhanin and J. M. Perales, "Stability of liquid bridges between equal disks in an axial gravity field," Phys. Fluids A **5**, 1305-1314 (1993).
2. D. Myshkis, V. G. Babskii, N. D. Kopachevskii, L. A. Slobozhanin and A. D. Tyuptsov, *Low-Gravity Fluid Mechanics* (Springer-Verlag, Berlin, 1987).
3. S. R. Coriell, S. C. Hardy and M. R. Cordes, "Stability of liquid zones", J. Colloid Interface Sci. **60**, 126 (1977).
4. L. H. Ungar and R. A. Brown, "The dependence of the shape and stability of captive rotating drops on multiple parameters", Philos. Trans. R. Soc. London Ser. A **306**, 347 (1982).
5. R. A. Brown and L. E. Scriven, "The shapes and stability of captive rotating drops", Philos. Trans. R. Soc. London Ser. A **297**, 51 (1980).
6. J. Lowry and P. H. Steen, "Capillary surfaces: stability from families of equilibria with application to the liquid bridge," Proc. R. Soc. London A **449**, 411-439 (1995).
7. Langbein, Crystal growth from liquid columns, J. Crys. Growth **104**, 47-59 (1990).
8. Tsamopolous, T. Chen, T. and A.Borkar, Viscous oscillations of capillary bridges, J. Fluid Mechanics, **235**, 579-609 (1992).
9. Mollot, J. Tsamopolous, T. Chen, and A. Ashgriz, Non-linear dynamics of capillary bridges: Experiments, J. Fluid Mech. **255**, 411-435 (1993).
10. G. Seebold, M. P. Hollister and H. M. Satterlee, "Capillary hydrostatics in annular tanks," J. Spacecraft **4**, No. 1, 101-105 (1967).
11. Salzman, Fluids management in space-based systems, Engineering, Construction and Operations in Space, 5th International Conference on Space, **1**, .521-526 (1966).
12. B. J. Ennis, J. Li, G. Tardos, and R. Pfeiffer, The influence of viscosity on the strength of an axially strained pendular bridge, Chem. Eng. Sci., **45**, 3071-3088 (1990).
13. V. P. Mehrota, and K.V.S. Sastry, Pendular bond strength between unequal-sized spherical particles, Powder tech., **25** 203-214 (1980).
14. L. A. Newhouse, and C. Pozrikidis, The capillary instability of annular layers and thin liquid threads, J. Fluid Mech., **242**, 193-209 (1992).
15. W. Keller and A. Mühlbauer, Floating Zone Silicon, in Preparation and Properties of Solid State Materials Vol. 5, W. R. Wilcox, ed. (Marcel Dekker, New York, 1981).
16. Mühlbauer, A. Muniznieks and J. Virbulis, Analysis of the dopant segregation effects at the floating zone growth of large silicon crystals, J. Crystal Growth, **180**, 372-380 (1997).
17. K. Brakke, Experimental Math. **1** 141- (1992).
18. J. I. D. Alexander, S. Delafontaine, A. Resnick and W. C. Carter, "Stability of non-axisymmetric liquid bridges," Microgravity Sci. Technol. **9**, 193-200 (1996).
19. L. A. Slobozhanin, J. I. D. Alexander and A. H. Resnick, "Bifurcation of the equilibrium states of a weightless liquid bridge," Phys. Fluids **9**, 1893-1905 (1997).
20. H. Resnick, "Experimental study of the dynamics and statics of nonaxisymmetric liquid bridges," Ph.D. Thesis, The University of Alabama in Huntsville, 1997.
21. L. A. Slobozhanin and J. I. D. Alexander, Stability of an isorotating liquid bridge in an axial gravity, Phys. Fluids **9**, 1880-1892 (1997).